European Journal of Neuroscience, Vol. 19, pp. 687–697, 2004

Simple spike and complex spike activity of floccular Purkinje cells during the optokinetic reflex in mice lacking cerebellar long-term depression

H. H. L. M. Goossens,[1,2,*] F. E. Hoebeek,[1,*] A. M. van Alphen,[1] J. van der Steen,[1] J. S. Stahl,[3] C. I. De Zeeuw[1] and M. A. Frens[1]
[1]Department of Neuroscience, Erasmus MC, Dr Molewaterplein 50, PO Box 1738, 3000 DR Rotterdam, the Netherlands
[2]Department of Biophysics, University of Nijmegen, Nijmegen, the Netherlands
[3]Department of Neurology, Case Western Reserve University, Cleveland, OH, USA

Keywords: cerebellar and vestibular nuclei, genetic manipulation, heterosynaptic plasticity, motor learning, vestibulo-ocular reflex

Abstract

Cerebellar long-term depression (LTD) at parallel fibre–Purkinje cell (P-cell) synapses is thought to embody neuronal information storage for motor learning. Transgenic L7-protein kinase C inhibitor (PKCI) mice in which cerebellar LTD is selectively blocked do indeed exhibit impaired adaptation in the vestibulo-ocular reflex (VOR) while their default oculomotor performance is unaffected. Although supportive, these data do not definitively establish a causal link between memory storage required for motor learning and cerebellar LTD. As the L7-PKCI transgene is probably activated from the early stages of P-cell development, an alternative could be that P-cells develop abnormal signals in L7-PKCI mutants, disturbing mechanisms of motor learning that rely on proper P-cell outputs. To test this alternative hypothesis, we studied simple spike (SS) and complex spike (CS) activity of vertical axis P-cells in the flocculus of L7-PKCI mice and their wild-type littermates during sinusoidal optokinetic stimulation. Both SS and CS discharge dynamics appeared to be very similar in wild-type and transgenic P-cells at all stimulus frequencies (0.05–0.8 Hz). The CS activity of all vertical axis cells increased with contralateral stimulus rotation and lagged ipsiversive eye velocity by 165–180°. The SS modulation was roughly reciprocal to the CS modulation and lagged ipsiversive eye velocity by ~15°. The baseline SS and CS discharge characteristics were indistinguishable between the two genotypes. We conclude that the impaired VOR learning in L7-PKCI mutants does not reflect fundamental aberrations of the cerebellar circuitry. The data thus strengthen the evidence that cerebellar LTD is implicated in rapid VOR learning but not in the development of normal default response patterns.

Introduction

Mechanisms of synaptic plasticity, such as long-term potentiation and long-term depression (LTD), are candidate mechanisms for information storage in the brain (e.g. Linden & Connor, 1995). A major goal in neuroscience is to understand how these mechanisms function in neural circuits that control learning in animal behaviour. The flocculus of the vestibulo-cerebellum is a crucial part of the reflex circuitry involved in the control and learning of compensatory eye movements, including the optokinetic and vestibulo-ocular reflex (OKR and VOR). More specifically, it has been hypothesized that learning in the VOR relies on LTD of the parallel fibre–Purkinje cell (P-cell) synapses driven by the coincidence of vestibular parallel fibre and visual climbing fibre signals (see, e.g. Ito, 1998 for review). This hypothesis represents a specific implementation of the general idea that synaptic plasticity in the cerebellar cortex is one of the major mechanisms of cerebellum-dependent motor learning.

Recent studies using various knockout mice have supported this theory by showing correlations between deficits in LTD and behavioural learning (Aiba *et al.*, 1994; Conquet *et al.*, 1994; Funabiki *et al.*, 1995; Kashiwabuchi *et al.*, 1995; Shibuki *et al.*, 1996). However, the interpretation of this work has suffered from the limitations that the knockout technique lacks anatomical and functional specificity of the genetically induced lesions. To overcome these limitations, we have previously created a transgenic mouse in which a protein kinase C inhibitory peptide, PKC(19–31), is selectively expressed in P-cells (De Zeeuw *et al.*, 1998). Both cerebellar LTD and adaptation of the VOR are impaired in these L7-PKC inhibitor (PKCI) mice while their default eye movement performance is unaffected (De Zeeuw *et al.*, 1998; Van Alphen & De Zeeuw, 2002; Gao *et al.*, 2003).

Although these data are consistent with LTD playing a role in actual memory storage, there is an alternative way of interpreting the results. It is possible that rapid motor learning is deficient in these mutants because the mutation disturbs the signal processing within the flocculus which, in turn, could disturb the learning process (see also Lisberger, 1998). To explore this possibility, we recently studied the spontaneous discharge of P-cells in the vermis and paramedian lobule of alert L7-PKCI mice and their wild-type littermates (Goossens *et al.*, 2001). It appeared that the simple spike (SS) and complex spike (CS) discharge properties of P-cells in L7-PKCI mice are normal, indicating that neither the activation of PKC nor the induction of LTD is essential for the normal baseline operation of the cerebellar circuitry.

Correspondence: Dr C. I. De Zeeuw, as above.
E-mail: C.DeZeeuw@erasmusmc.nl

*H.H.L.M.G. and F.E.H. contributed equally.

Received 9 October 2003, accepted 1 December 2003

doi:10.1111/j.1460-9568.2003.03173.x

However, these results do not rule out the possibility that the neural signals in the flocculus of the cerebellum, which are known to be related to the control and learning of compensatory eye movements, are abnormal in LTD-deficient animals. In fact, very little is known about these signals even for wild-type mice. As the L7-PKCI transgene is probably activated from the early stages of P-cell differentiation and maturation (De Zeeuw *et al.*, 1998), it could well be that a normal development of P-cell responsiveness to parallel fibre and/or climbing fibre signals is not possible in the L7-PKCI mutant. Clearly, if the P-cell output was abnormal, it could disturb mechanisms of synaptic plasticity that rely either directly or indirectly on proper P-cell signals. This possibility complicates interpretation of the relation between LTD blockade and motor learning behaviour.

To test whether P-cell signals are disturbed in the LTD-deficient L7-PKCI mutant, we studied the SS and CS discharge properties of P-cells in the flocculus of L7-PKCI mice and their wild-type littermates during the OKR.

Materials and methods

Animal preparation

Data were collected from heterozygous transgenic L7-PKCI mice and their wild-type littermates (C57BL/6 mouse strain background; 3–12 months old). In the L7-PKCI mouse, the pseudo substrate PKC inhibitor, PKC(19–31), is selectively expressed in P-cells under the control of the pcp-2(L7) gene promoter. The animals were prepared for chronic neurophysiological experiments under halothane anaesthesia using procedures described recently (Goossens *et al.*, 2001). In short, a head holder was implanted on the scull and a recording chamber was placed over a small hole in the cerebellar cranium. In addition, all mice received a search coil implant for recording of eye position (see Van Alphen *et al.*, 2001 for details). During an experiment, the animal was immobilized in a custom restrainer by bolting the head holder to a head fixation post. Head orientation was such that the horizontal semicircular canals were in the horizontal plane (plane of nasal bone tipped approximately 35° down). All experiments were conducted in accordance with the European Communities Council Directive of November 24, 1986 (86/609/EEC) and were reviewed and approved by the local ethics committee of the Erasmus University Rotterdam.

Optokinetic stimulation

A panoramic stimulus was used for binocular visual stimulation. The stimulus consisted of a random-dot pattern that was back-projected on a translucent cone-shaped dome surrounding the mouse. To generate stimulus rotations about the vertical axis running through the centre of the animal's interaural line, the projection system was equipped with a servomotor that could rotate a slide in front of the lens. Stimulus position was measured and controlled by a 1401plus unit (Cambridge Electronic Design Ltd, Cambridge, UK). We used sinusoidal stimuli consisting of at least 10 continuous cycles and lasting at least 120 s. Stimulus amplitude was $\pm 5^\circ$ and frequencies were 0.05, 0.1, 0.2, 0.4 and 0.8 Hz. In this manner, peak velocities ranged from 1.5 to 25°/s. In a few animals, the OKR was also tested at 0.025 and 1.6 Hz.

Eye movement recordings

The position of the left eye was measured with the magnetic induction method using miniature coils that were implanted on the lateral side of the eye (Van Alphen *et al.*, 2001). Eye position signals were sampled at 500 Hz (1401plus; Cambridge Electronic Design Ltd) and stored on disk for off-line analysis using Spike 2 (Cambridge Electronic Design Ltd). The horizontal component of the eye position signal was calibrated by rotating the magnetic field $\pm 10^\circ$ about the vertical axis running through the centre of the animal's interaural line.

Single cell recordings

Extracellular activity was recorded with glass micropipettes that were advanced into the left flocculus by a hydraulic microdrive equipped with a stepping motor (see Goossens *et al.*, 2001 for details). The raw electrode signal was amplified, filtered, digitized and stored on disk for off-line analysis. Single unit P-cell activity was identified by the presence of a brief pause in SS discharge after a CS and was carefully monitored during the course of a recording. Once a P-cell was isolated, its preferred axis of rotation was determined by monitoring its CS activity while moving a random dot pattern in various directions (Simpson *et al.*, 1988). Between recording sessions the brain was covered by a silastic sheet and the chamber was sealed.

Histology

The anatomical locations of the recording sites were marked either by methylene blue injections or by electrolytic lesions. The animals were deeply anaesthetized with pentobarbital sodium and transcardially perfused with saline followed by 4% formalin. Sagittal slices of the brainstem and cerebellum (50 μm thick) were prepared and stained according to standard histological procedures. Inspection of successive slices at the light microscopic level confirmed that all recording sites were located within the flocculus (see Fig. 1).

Data analysis

Off-line analysis was performed in Matlab (Mathworks Inc., Natick, MA, USA). Eye velocity was calculated from the calibrated eye position data and quick phases were removed. Gain and phase of the eye movements relative to the stimulus were determined by fitting sine functions to the slow-phase eye velocity traces. The response gain was defined as the ratio between the (fitted) amplitudes of the eye velocity and stimulus velocity traces.

The SS and CS were detected and discriminated with custom software that clustered groups of spikes by means of a linear discriminant analysis on the first four principal components of the spike wave forms (see e.g. Eggermont, 1990). Histograms of SS triggered on the occurrence of a CS were made (bin width 1 ms) to verify that each isolated P-cell showed a clean climbing fibre pause (Simpson *et al.*, 1996). Lack of a pause was taken to indicate that the cell was not a P-cell or that isolation was imperfect. Spontaneous activity of each P-cell was characterized by (i) the mean SS and CS firing rate; (ii) the SS and CS coefficient of variance and (iii) the climbing fibre pause duration (see also Goossens *et al.*, 2001).

The P-cells that showed optimal CS modulation for stimulus rotations about the vertical axis were selected for further analysis. Peristimulus time histograms were made to evaluate modulation of the SS and CS discharge (48 and 24 bins/cycle, respectively) where quick-phase epochs were discarded. The percentage of SS modulation amplitude, A, was determined using Fourier analysis

$$A = a_1/a_0 \times 100\%$$

where a_0 is the mean firing rate and a_1 the amplitude at fundamental frequency, f. To further assess whether wild-type and mutant P-cells generate different responses in relation to the actual OKR movements, the SS and CS firing rates (F) were both quantified as a function of eye position (E) and eye velocity (E')

$$F(t) = kE(t) + rE'(t) + c \quad \text{for } F(t) > 0$$
$$F(t) = 0 \quad \text{otherwise}$$

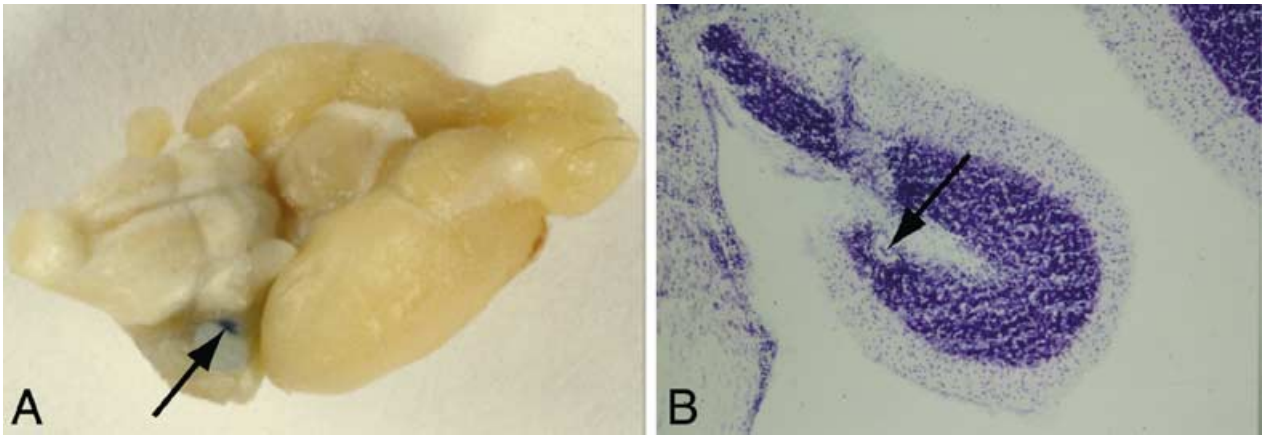

FIG. 1. Histology of the recording sites confirmed that the recordings were from floccular Purkinje cells. (A) Injection of methylene blue at one of the recording sites in a C57BL/6 mouse. (B) Sagittal slice of brainstem and cerebellum of an L7-protein kinase C inhibitor mouse with electrolytic lesions along an electrode track through the flocculus.

where t denotes time (s), k denotes apparent eye position sensitivity (spk/s/$^\circ$) and r is the apparent eye velocity (spk/s per $^\circ$/s) (Stahl & Simpson, 1995). The least squares criterion was used to determine the best-fit parameters. Unlike the Fourier analysis, this procedure provides a convenient way to quantify the P-cell discharge because it can account for complete suppression of the discharge at a particular phase of the response (see Fig. 2 for illustration) and because it allows quick-phase epochs to be excluded. Note, however, that by correlating the P-cell activity with various components of the eye movement we do not mean to imply a causal linkage. The sensitivity parameters merely serve as a tool to quantify possible differences between wild-type and mutant P-cell responses taking into account the animal's actual eye movement behaviour. Statistical evaluation of the fit results indicated significant SS and CS modulation for all identified vertical axis P-cells (VA-cells) ($P < 0.01$; Pearson's correlation coefficients typically >0.75). The phase of the firing rate with reference to ipsiversive eye velocity (θ) at each stimulus frequency (f) was obtained from

$$\theta = \arctan[k/2\pi f.r)].$$

Phase leads were taken as positive and phase lags as negative. The magnitude sensitivity (M), which is the ratio of the amplitudes of firing rate and eye position, was calculated from the relation:

$$M = \sqrt{[2\pi f.r)^2 + k^2}].$$

Statistical analysis of the data included nonorthogonal (i.e. 'unequal n') two-factor analysis of variance (ANOVA) and unpaired Student's t-tests (two-tailed) to evaluate differences in means as well as non-parametric Wilcoxon rank-sum tests for comparison of medians. Kolmogorov–Smirnov and Kuiper tests were used to evaluate differences in empirical distribution functions (see e.g. Press *et al.*, 1992). Significance levels (P) are indicated in the text. To determine whether violations of the normality assumption and heteroscedasticity of the data affected the outcomes of the ANOVAs, we also used a two-factor ANOVA by ranks in an extension of the Kruskal–Wallis test called the Scheirer–Ray–Hare test (Scheirer *et al.*, 1976). The results of these tests are not shown as the outcomes of the classical ANOVAs proved to be valid in all cases. To augment the traditional hypothesis testing approach, 95% confidence intervals (CI, two-sided) of the differences between the two genotypes are reported to indicate upper and lower limits of the observed differences. As data were not normally distributed, these 95% CIs were estimated with the use of a Monte Carlo bootstrap procedure in which the observations were resampled 10 000 times (with return).

Results

We recorded single unit activity of P-cells in the flocculus of L7-PKCI transgenic mice ($n = 7$) and their wild-type littermates ($n = 7$). Simultaneous records of SS and CS activity were obtained from 54 wild-type and 44 mutant P-cells. Histology of recording sites confirmed that the isolated P-cells were located within the flocculus (see Fig. 1).

Spontaneous Purkinje cell activity

Spontaneous activity of floccular P-cells was recorded for about 2–3 min in the light. Table 1 summarizes the results. Note that both the mean SS firing rates (~ 60 spk/s) and mean CS firing rates (~ 0.9 spk/s) were very similar between wild-type and L7-PKCI P-cells. Statistical analysis indicated that neither the SS firing rates nor the CS firing rates were significantly different between the two P-cell populations (Student's t-test, $P > 0.2$; Wilcoxon rank-sum test, $P > 0.2$). The temporal jitter in the spontaneous SS and CS discharge, as quantified by the coefficient of variance, was also not significantly different between the two P-cell populations (Student's t-test, $P > 0.1$; Wilcoxon rank-sum test, $P > 0.3$). Average values for the SS as well as the CS coefficient of variance were ~ 0.7 in both genotypes (Table 1). The average duration of the climbing fibre pause was ~ 13 ms in both wild-type and mutant P-cells (not significantly different; Student's t-test, $P > 0.3$; Wilcoxon rank-sum test, $P > 0.2$). The right-hand column of Table 1 lists the 95% CI for the differences between the two genotypes to indicate the sampling allowances for these observations. For each parameter, we also examined possible differences in its empirical distribution function using two-sample Kolmogorov–Smirnov and Kuiper tests but no significant differences between the two genotypes were found ($P > 0.3$ for all six parameters and for both types of test).

Eye movements

The gain and phase of the optokinetic eye movement responses of the wild-type and L7-PKCI mice used in this study were in the same range as those previously observed by Van Alphen *et al.* (2001, 2002). With stimulus amplitude fixed at $\pm 5^\circ$, the average gain of the OKR gradually decreased from about 0.35 at 0.025–0.05 Hz to approximately 0.02 at 1.6 Hz (Fig. 3). The phase of the eye velocity with reference to stimulus velocity (relative to the head) ranged from an average lead of

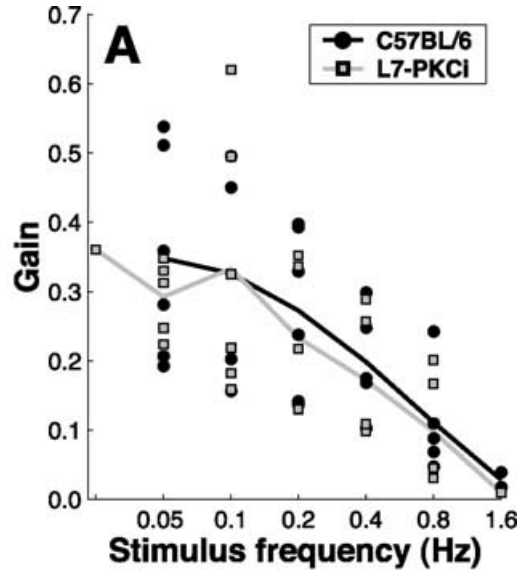

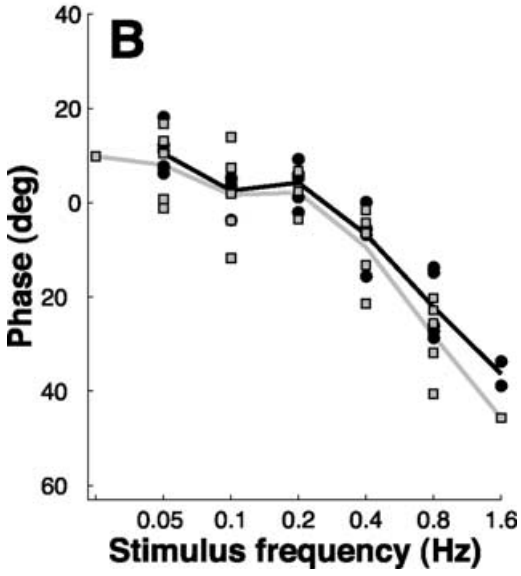

FIG. 2. Simple spike (SS) and complex spike (CS) responses of a typical vertical axis Purkinje cell in the flocculus of (A) a C57BL/6 wild-type and (B) an L7-protein kinase C inhibitor (PKCI) mouse (B) to sinusoidal optokinetic stimulation (OKS) at three different frequencies (0.05, 0.2 and 0.8 Hz; $\pm 5^\circ$ amplitude). Top row, velocity of the OKS and eye velocity (Eye) in world coordinates (ipsiversive motion is positive). Thick lines are sine fits to the eye movement data. Middle and bottom row, peristimulus time histograms of SS and CS activity, respectively. Thick lines are data fits of the (conditional) firing rate as a function of measured eye position and eye velocity (see Materials and methods and Results).

about 10° at 0.025–0.05 Hz to an average lag of about 35° at 1.6 Hz (Fig. 3).

Response patterns of vertical axis Purkinje cells

Of all 98 P-cells recorded in this study, 39 wild-type and 36 transgenic cells were identified as VA-cells and could be tested in further detail during vertical axis optokinetic stimulation. The CS discharge of the remaining 23 P-cells showed optimal sensitivity for stimulus rotations about the horizontal axis orientated at 135° ipsilateral azimuth. In line

TABLE 1. Spontaneous Purkinje cell (P-cell) activity

	C57BL/6 ($n = 34$)	L7-PKCI ($n = 33$)	Difference (95% CI)
Simple spikes			
Mean firing rate (spk/s)	55 ± 20	59 ± 19	(−5, 13)
Coefficient of variance	0.7 ± 0.3	0.7 ± 0.2	(−0.1, 0.1)
Complex spikes			
Mean firing rate (spk/s)	0.9 ± 0.4	0.8 ± 0.3	(−0.3, 0.1)
Coefficient of variance	0.8 ± 0.2	0.7 ± 0.1	(−0.1, 0.1)
Climbing fibre pause (ms)	12 ± 9	14 ± 7	(−2, 6)

Parameters of spontaneous simple spike and complex spike activity of floccular P-cells in C57BL/6 wild-type and L7-protein kinase C inhibitor (PKCI) mutant mice (expressed as mean $\pm$ SD) and 95% confidence intervals (CI) for the differences between the two genotypes (estimated with Monte Carlo bootstrap).

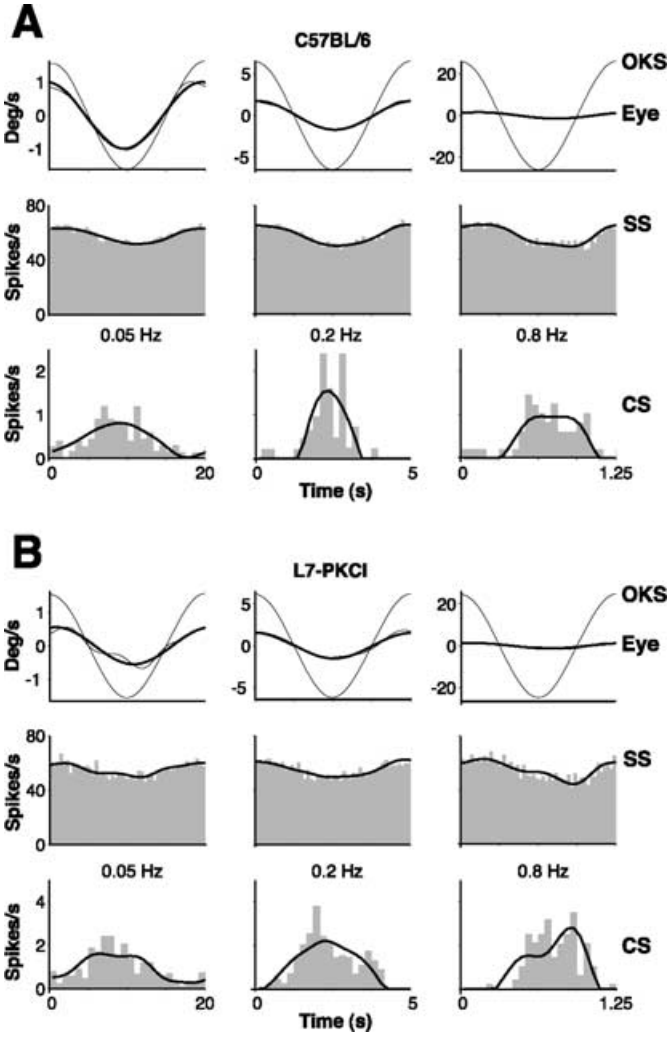

FIG. 3. (A) Gain and (B) phase of the optokinetic reflex responses of the C57BL/6 wild-type mice ($n = 7$) and the L7-protein kinase C inhibitor (PKCI) transgenic mice ($n = 7$) used in this study. Phase leads relative to the stimulus are positive. Each symbol represents the (mean) response of an individual animal. Solid lines are the average values for each genotype. Note very similar gain and phase relations for the two genotypes.

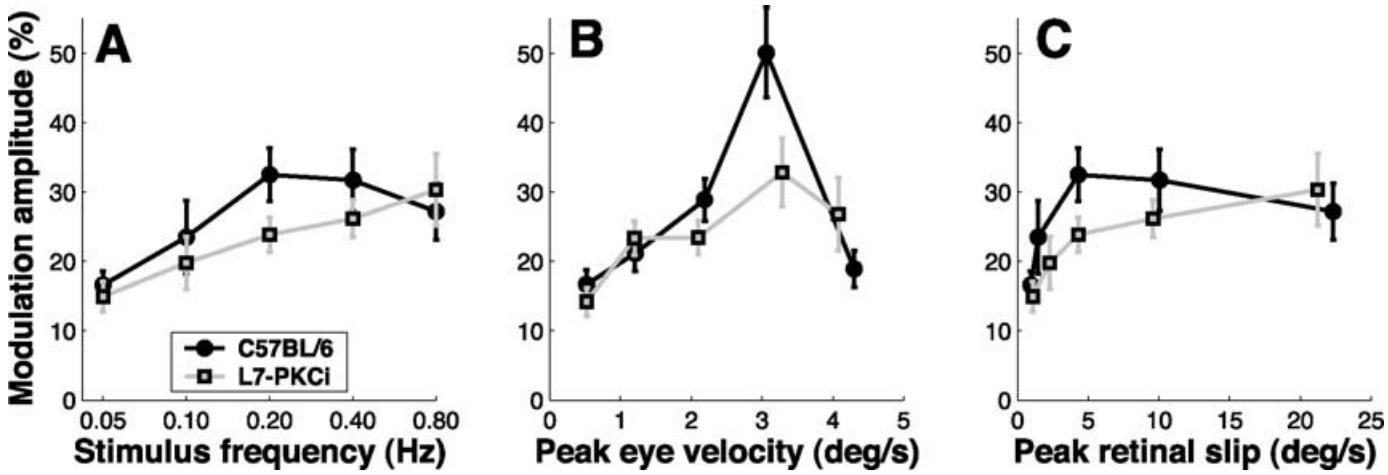

FIG. 4. Mean percentage of simple spike modulation amplitude as a function of (A) stimulus frequency, (B) peak eye velocity and (C) peak retinal slip velocity. In A and C, responses were averaged per stimulus frequency. 95% confidence intervals (CI) for the differences between C57BL/6 and L7-protein kinase C inhibitor (PKCI) Purkinje cells at 0.05–0.8 Hz are $\Delta A_{0.05} = (-7, 4)$, $\Delta A_{0.1} = (-16, 8)$, $\Delta A_{0.2} = (-17, 1)$, $\Delta A_{0.4} = (-16, 4)$ and $\Delta A_{0.8} = (-9, 16)$%, where the subscripts refer to stimulus frequency. In (B), data were binned according to the measured peak eye velocity (bin width 1°/s). 95% CI for the differences between the two genotypes in each velocity bin are $\Delta A_{0.5} = (-7, 3)$, $\Delta A_{1.2} = (-5, 9)$, $\Delta A_{2.1} = (-13, 2)$, $\Delta A_{3.2} = (-32, 2)$ and $\Delta A_{4.2} = (-2, 18)$%, where the subscripts refer to peak eye velocity (°/s, average between wild-type and mutant). Note very similar response curves for the two genotypes. Error bars, ± 1 SEM.

with the modular organization of the cerebellum, the two types of P-cells were reproducibly encountered at distinctly different locations (as inferred from successive penetrations in the same animal) in both genotypes.

Figure 2 illustrates the SS and CS discharge of a typical wild-type (Fig. 2A) and mutant (Fig. 2B) VA-cell during optokinetic stimulation at three different frequencies (0.05, 0.2 and 0.8 Hz). Note that the response patterns of the two cells are qualitatively similar. In line with the response patterns typically seen in floccular VA-cells from other species, such as the rabbit (e.g. De Zeeuw *et al.*, 1995; Simpson *et al.*, 1996; Frens *et al.*, 2001), CS activity increased during contralateral stimulus rotation and was strongly inhibited during ipsilateral motion. The SS activity, on the other hand, increased with ipsilateral stimulus rotation and decreased during contralateral rotation, resulting in a temporally reciprocal relation between SS and CS modulation. Both eye velocity and SS modulation were approximately in phase with stimulus velocity at 0.05 and 0.2 Hz but clearly lagged stimulus velocity at 0.8 Hz. A similar phase shift can be observed in the CS activity of both cells. Complete suppression of CS activity during ipsilateral stimulus rotation was often observed at stimulus frequencies >0.1 Hz. Complete cessation of SS activity was rare under all stimulus conditions.

Cells that showed an increase in SS firing for contralateral stimulus motion were frequently observed but they could not be identified as VA-cells. Either they showed no pause in SS activity after the CS or their CS activity was optimally modulated by visual world rotation about the ipsilateral 135° axis in the horizontal plane (Graf *et al.*, 1988).

Simple spike discharge dynamics

Figure 4 quantifies the percent modulation amplitude (see Materials and methods) of the SS discharge as a function of stimulus frequency (Fig. 4A), maximum eye velocity (Fig. 4B) and maximum retinal slip velocity (Fig. 4C). As can be observed in Fig. 4A, the SS modulation amplitude for wild-type vs. transgenic P-cells was very similar at each stimulus frequency (Wilcoxon rank-sum tests, $P > 0.1$, Kuiper tests, $P > 0.2$ at all frequencies). In both genotypes, the SS modulation amplitude tends to increase with increasing stimulus frequency from about 15% at 0.05 Hz to about 30% at 0.8 Hz. Further analysis of these data with a two-factor ANOVA confirmed that there was a significant main effect of stimulus frequency ($F_{4,175} = 3.60$, $P < 0.01$). In addition, genotype ($F_{1,175} = 1.35$, $P > 0.2$) and interaction terms ($F_{4,175} = 0.66$, $P > 0.6$) were not significant, indicating that the two response curves in Fig. 4A are not significantly different. To augment these findings, 95% CI for the differences between the two genotypes at each stimulus frequency are indicated in the legend. As shown in Fig. 4B, the relation between SS modulation amplitude and maximum eye velocity was also similar between the two genotypes (not significantly different; two-factor ANOVA, $F_{1,175} = 1.30$, $P > 0.2$; Wilcoxon rank-sum tests, $P > 0.05$; Kuiper tests, $P > 0.2$ at all velocity bins; minor differences in ordinate value per bin not taken into account). In both genotypes, the SS modulation amplitude tends to be greatest at about 3°/s (significant main effect of maximum eye velocity; $F_{4,175} = 11.01$, $P < 0.0001$). Figure 4C re-plots the average SS modulation amplitudes from Fig. 4A as a function of the average maximum retinal slip velocity at each frequency. Although the ordinate values are slightly different in this case (as in Fig. 4B), it can be inferred from the error bars (indicating ± 1 SEM) that the values for mutants fall within the 95% CI estimated for the control curve (about 2 × SEM), indicating that these response curves are also not significantly different between wild-type and L7-PKCI P-cells (see analysis Fig. 4A for two-factor ANOVA).

Interpretation of the above results is somewhat complicated by the variability in the eye movement responses, both within and across individual animals (see Fig. 3). To circumvent this problem, the SS modulation was analysed as a function of eye position and eye velocity (see Materials and methods). As is illustrated for the P-cell responses in Fig. 2, this analysis procedure yielded a good description of SS modulation (thick lines, middle rows in A and B; correlation between data and model >0.75). Apparent eye position [k (spk/s/°)] and eye velocity [r (spk/s per °/s)] sensitivities fitted to the SS data from the wild-type VA-cell (Fig. 2A) were $(k, r)_{0.05} = (0.86, 5.16)$, $(k, r)_{0.2} = (0.92, 4.46)$ and $(k, r)_{0.8} = (1.35, 5.58)$, where the subscripts refer to stimulus frequency. For the L7-PKCI cell (Fig. 2B), these values were $(k, r)_{0.05} = (-0.59, 8.98)$, $(k, r)_{0.2} = (0.29, 3.95)$ and $(k, r)_{0.8} = (13.9, 5.05)$. As indicated in Materials and methods, the r- and k-values were

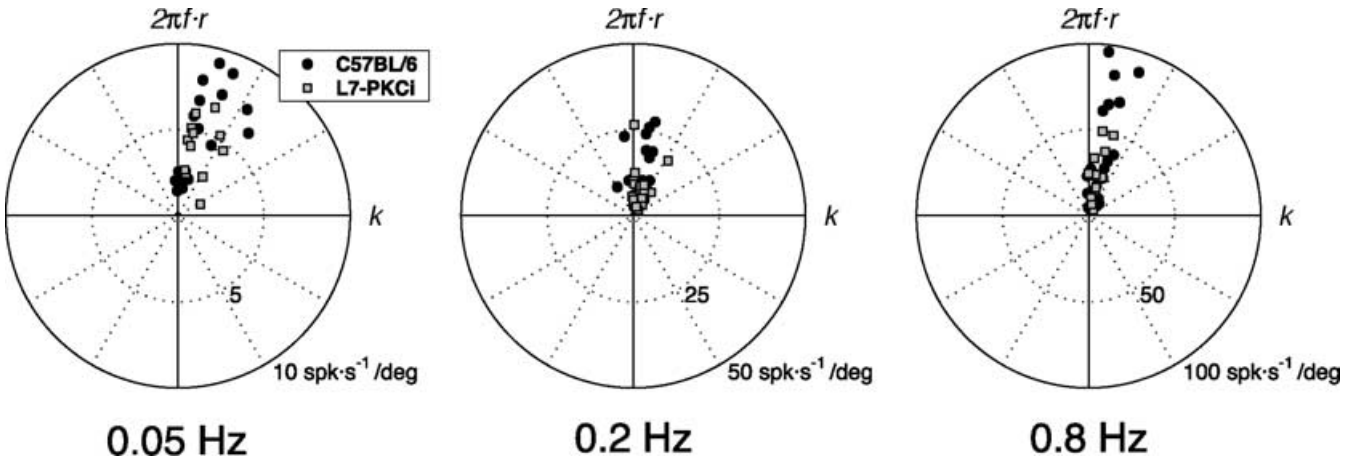

FIG. 5. Polar plots of simple spike (SS) phase and SS magnitude sensitivity of individual Purkinje cells in wild-type and mutant mice during optokinetic stimulation at 0.05, 0.2 and 0.8 Hz. Horizontal and vertical axis represent k and $2\pi f{\cdot}r$-values, respectively. The phase of SS modulation with reference to eye velocity is indicated by the angle with the vertical axis, whereas the magnitude sensitivity corresponds to the radial distance from the centre of the plot. Note scaling differences.

subsequently used to calculate the SS magnitude sensitivity (M) and the phase (θ) of the SS modulation in reference to eye velocity. A prerequisite for a valid comparison of SS responses in wild-type and mutant P-cells on the basis of these parameters is, of course, that the model describes the responses equally well in both genotypes. Analysis of Pearson's correlation between data and model fit indicated that the goodness of fit was indeed similar between the two P-cell populations (not significantly different; ANOVA, $F_{1,175} = 1.28$, $P > 0.25$; typically correlations >0.75). Note that this is not trivial because, in the mutant, the SS responses could have been much noisier or somehow more distorted due to possible aberrations of the cerebellar circuitry.

Figure 5 shows polar scatter plots of the SS phase and magnitude sensitivity of all individual VA-cells tested during optokinetic stimulation at 0.05, 0.2 and 0.8 Hz. In this type of plot, the horizontal and vertical axis represent k (eye position component) and $2\pi f{\cdot}r$ (eye velocity component), respectively. The phase of SS modulation with reference to eye velocity is, therefore, indicated by the angle with the vertical axis, whereas the magnitude sensitivity corresponds to the radial distance from the centre of the plot. Note that the SS responses of all VA-cells lie in the top two quadrants, signifying that their SS firing rate increased during ipsilateral eye rotation. Furthermore, the SS responses of wild-type and transgenic P-cells are largely overlapping. Statistical analysis of these scatter plots with a two-dimensional Kolmogorov–Smirnov test indicated that the location and shape of the two-dimensional distributions of k- vs. r-values were not significantly different between the two genotypes at all five stimulus frequencies ($P > 0.4$). To further scrutinize these results, subsequent analyses focused on the respective Cartesian (k- and r-values) and polar (M and θ) coordinates of the data.

Table 2 lists the average k- and r-values for the wild-type and transgenic P-cell population for all five stimulus frequencies. Note that, for wild-type VA-cells, k gradually increases from 1.41 spk/s/° at 0.05 Hz to 7.58 spk/s/° at 0.8 Hz, whereas r drops from 14.6 spk/s per °/s at 0.05 Hz to 6.51 spk/s per °/s at 0.8 Hz. Very similar results were obtained in the L7-PKCI P-cell population. Two-factor ANOVA indicated that neither k nor r was significantly influenced by genotype ($F_{1,175} = 0.73$, $P > 0.3$ and $F_{1,175} = 1.57$, $P > 0.2$, respectively) and that there was a significant main effect of stimulus frequency on k ($F_{4,175} = 12.16$, $P < 0.0001$) as well as r ($F_{4,175} = 11.84$, $P < 0.0001$). Interaction terms were not significant ($F_{4,175} = 1.21$, $P > 0.3$ and $F_{4,175} = 0.28$, $P > 0.8$, respectively). Wilcoxon rank-sum tests and Kuiper tests further supported the conclusion that there were no significant differences in the k- and r-values between the two genotypes ($P > 0.2$ at all stimulus frequencies). The average baseline of the SS firing rate, as quantified by the c-parameter (not listed), was ~60 spk/s in both genotypes (no significant differences; two-factor ANOVA, $F_{1,175} = 0.17$, $P > 0.6$) and did not vary as a function of stimulus frequency ($F_{4,175} = 1.13$, $P > 0.3$).

Figure 6 quantifies the average magnitude sensitivity of the SS responses and the average phase of the SS discharge with reference to eye velocity as a function of stimulus frequency as calculated from

TABLE 2. Regression results of simple spike (SS) modulation

	Stimulus frequency				
	0.05 Hz	0.1 Hz	0.2 Hz	0.4 Hz	0.8 Hz
C57BL/6					
k (spk/s/°)	1.41 ± 0.34	1.34 ± 0.34	1.89 ± 0.48	2.91 ± 0.54	7.58 ± 1.46
r (spk/s per °/s)	14.6 ± 2.00	7.33 ± 1.72	7.96 ± 1.14	6.41 ± 0.84	6.51 ± 1.15
n	17	15	28	26	23
L7-PKCI					
k (spk/s/°)	1.23 ± 0.22	0.56 ± 0.24	2.05 ± 0.46	3.67 ± 0.75	5.02 ± 1.19
r (spk/s per °/s)	12.5 ± 1.51	7.21 ± 1.26	6.09 ± 0.87	4.60 ± 0.61	4.74 ± 0.86
n	12	10	23	19	12

Apparent eye position sensitivity (k) and apparent eye velocity sensitivity (r) for SS responses of floccular Purkinje cells in C57BL/6 wild-type and L7-protein kinase C inhibitor (PKCI) mutant mice. Values of k and r are expressed as mean ± SEM.

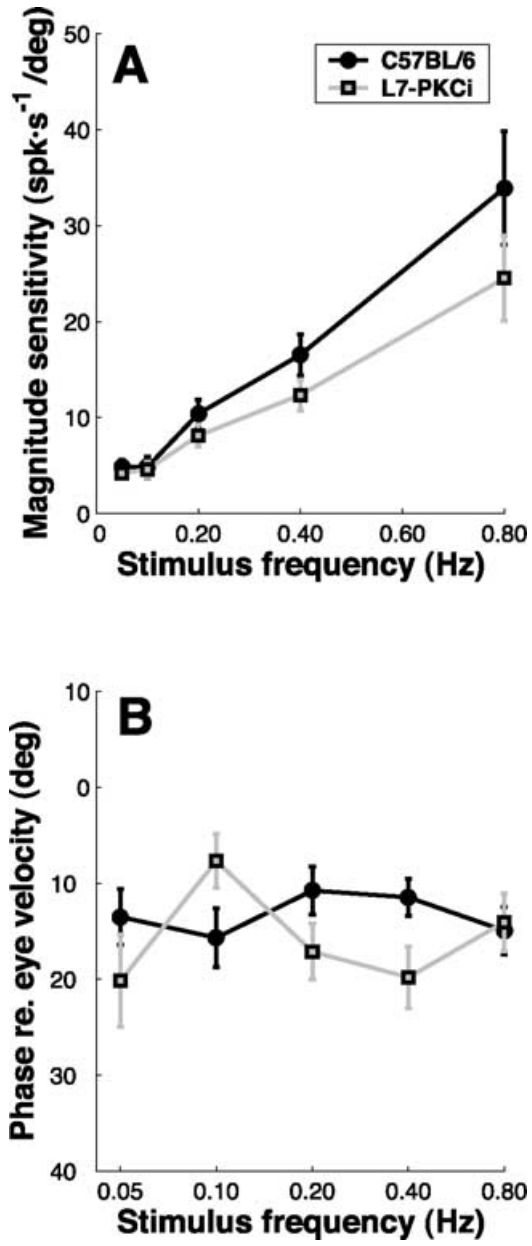

FIG. 6. (A) Magnitude sensitivity and (B) phase of the simple spike discharge for wild-type and L7-protein kinase C inhibitor (PKCI) Purkinje cells (P-cells) as a function of stimulus frequency. Error bars, ± 1 SEM. Note very similar sensitivity and phase relations for the two genotypes. 95% confidence intervals (CI) for the difference between magnitude sensitivities in wild-type and L7-PKCI P-cells are $\Delta M_{0.05} = (-2, 1)$, $\Delta M_{0.1} = (-3, 2)$, $\Delta M_{0.2} = (-6, 2)$, $\Delta M_{0.4} = (-9, 2)$ and $\Delta M_{0.8} = (-23, 5)$ spk/s/°. 95% CI for the phase differences between the two genotypes are $\Delta\theta_{0.05} = (-17, 3)$, $\Delta\theta_{0.1} = (-2, 15)$, $\Delta\theta_{0.2} = (-13, 2)$, $\Delta\theta_{0.4} = (-15, 2)$, $\Delta\theta_{0.8} = (-7, 8)°$.

the *k*- and *r*-values (see Materials and methods). The 95% CI of the differences between the two genotypes are indicated in the legend. Note that the magnitude sensitivity of the SS responses increases from about 4 spk/s/° at 0.05 Hz to about 30 spk/s/° at 0.8 Hz in both P-cell populations (Fig. 6A). Accordingly, two-factor ANOVA of these data indicated a significant main effect of stimulus frequency ($F_{4,175} = 23.53$, $P < 0.0001$) and, in line with the Kolmogorov–Smirnov analysis of the scatter plots in Fig. 5, differences between the two genotypes were not statistically significant ($F_{1,175} = 2.30$, $P > 0.1$). The latter conclusion was also sustained by Wilcoxon rank-sum tests and Kuiper tests comparing the SS magnitude sensitivities of wild-type and mutant P-cells at each stimulus frequency ($P > 0.2$ at all stimulus frequencies). As illustrated by the raw data in Fig. 2, the SS modulation was roughly in phase with eye velocity even though there were substantial changes in the phase of the OKR with reference to the stimulus. As shown in Fig. 6B, this behaviour was consistent across the population of recorded P-cells; the average phase lag of the SS modulation with reference to eye velocity was only about −15° at all stimulus frequencies in both genotypes. Evaluation of these data with a two-factor ANOVA indicated that the SS phase curves in Fig. 6B were not significantly different between the two genotypes ($F_{4,175} = 0.50$, $P > 0.7$) and that stimulus frequency ($F_{1,175} = 2.12$, $P > 0.1$) as well as interaction terms ($F_{4,175} = 1.86$, $P > 0.1$) were also not significant. Comparing the phase of the SS modulation in wild-type and mutant P-cells by the use of Wilcoxon rank-sum tests and Kuiper tests at each stimulus frequency also revealed no significant differences between the two P-cell populations ($P > 0.4$ at all stimulus frequencies).

Complex spike discharge dynamics

The CS firing rate modulation was analysed in a similar fashion as the SS discharge, i.e. as a function of eye position and eye velocity. Typical results obtained with this procedure are shown in Fig. 2 (thick lines, bottom rows in A and B; correlation between data and fit >0.77). *k*- and *r*-values fitted to the CS responses of the wild-type VA-cell (Fig. 2A) were $(k, r)_{0.05} = (0.04, -0.38)$, $(k, r)_{0.2} = (0.37, -1.34)$ and $(k, r)_{0.8} = (0.60, -0.48)$ and for the L7-PKCI cell (Fig. 2B) $(k, r)_{0.05} = (0.32, -1.01)$, $(k, r)_{0.2} = (0.32, -0.85)$ and $(k, r)_{0.8} = (-1.17, -1.07)$. Across all recordings, goodness of fit was similar between the two P-cell populations (not significantly different; two-factor ANOVA, $F_{1,175} = 1.28$, $P > 0.35$; correlations between data and fit typically >0.75). The scatter plots in Fig. 7 illustrate the fit results for all individual VA-cells tested during optokinetic stimulation at 0.05, 0.2 and 0.8 Hz. Note that the CS responses fall in the bottom two quadrants, signifying that the CS firing rate of all VA-cells increased during contralateral eye rotation. Analysis of these scatter plots with a two-dimensional Kolmogorov–Smirnov test indicated that the location and shape of the distributions of *k*- vs. *r*-values were not significantly different between the two genotypes for all stimulus frequencies ($P > 0.05$), except at 0.2 Hz ($P = 0.03$) where the orientation of the distribution for CS responses in L7-PKCI cells is slightly shifted in an anticlockwise direction with respect to the wild-type data.

Table 3 summarizes the average *k*- and *r*-values of the CS discharge for wild-type and transgenic P-cells. Note that both the *k*- and *r*-values were significantly influenced by stimulus frequency (two-factor ANOVA; $F_{4,175} = 18.86$, $P < 0.0001$ and $F_{4,175} = 4.57$, $P < 0.002$, respectively). In both genotypes, the average *k*-value gradually increased with stimulus frequency from 0 spk/s/° at 0.05 Hz to about 0.75 spk/s/° at 0.8 Hz. The average *r*-value gradually changed from about −0.5 spk/s per °/s at the two lowest frequencies to about −0.95 spk/s per °/s at 0.8 Hz. However, neither *k*- nor *r*-values were significantly different between wild-type and transgenic P-cells ($F_{1,175} = 1.38$, $P > 0.2$ and $F_{1,175} = 1.21$, $P > 0.2$, respectively) and interactions were absent ($F_{4,175} = 0.5$, $P > 0.7$ and $F_{4,175} = 0.69$, $P > 0.5$, respectively). Comparing the *k*- and *r*-values with the use of Wilcoxon rank-sum tests and Kuiper tests at each stimulus frequency also revealed no significant differences between the two P-cell populations ($P > 0.2$ at all stimulus frequencies).

Figure 8 quantifies the average magnitude sensitivity of the CS responses and the average phase of the CS discharge with reference to eye velocity as a function of stimulus frequency. In both P-cell populations, the magnitude sensitivity of the CS discharge gradually

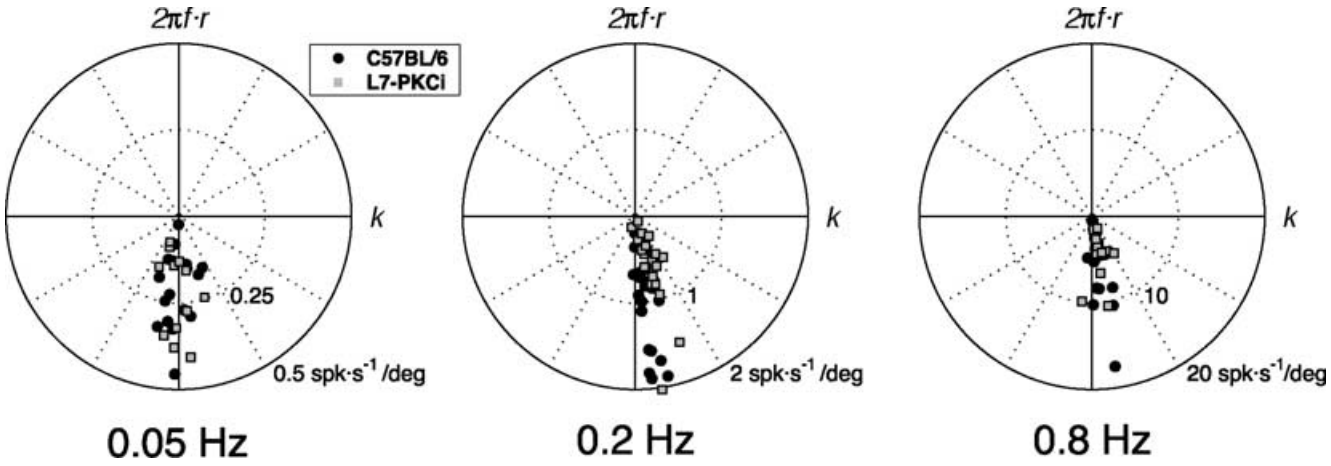

FIG. 7. Polar plots of complex spike (CS) phase and CS magnitude sensitivity of individual wild-type and mutant Purkinje cells (P-cells) during optokinetic stimulation at 0.05, 0.2 and 0.8 Hz. Note that CS responses of all cells lie in the bottom two quadrants, signifying that the CS firing rate of vertical axis P-cells increased during contralateral eye rotation.

increased from about 0.2 spk/s/° at 0.05 Hz to about 4.5 spk/s/° at 0.8 Hz (Fig. 8A; not significantly different between genotypes; two-factor ANOVA, $F_{1,175} = 0.13$, $P > 0.7$; Wilcoxon rank-sum and Kuiper tests, $P > 0.3$ at all stimulus frequencies). Whereas the phase of the SS discharge with reference to eye velocity remained constant, the phase of the CS discharge showed a small, but significant, change as a function of stimulus frequency (Fig. 8B; two-factor ANOVA, main effect, $F_{4,175} = 13.91$, $P < 0.0001$). There were also some subtle differences between wild-type and mutant P-cells (significant main effect, $F_{1,175} = 12.86$, $P < 0.0005$; no significant interactions, $F_{4,175} = 1.56$, $P > 0.1$). The 95% CI of these differences are listed in the legend. At 0.05 Hz, CS modulation was almost perfectly in counter phase with eye velocity in both genotypes (not significantly different; Student's *t*-test, $P = 0.6$; Wilcoxon rank-sum test, $P = 0.9$). At the higher frequencies, however, CS modulation in wild-type VA-cells lagged eye velocity by about −170° while the average phase lag in transgenic VA-cells was reduced to about −165° at 0.2 and 0.4 Hz (Student's *t*-tests, $P < 0.004$; Wilcoxon rank-sum test, $P < 0.0002$).

The results presented above suggested that the phase of the CS modulation with reference to the SS discharge might be slightly different between wild-type and mutant P-cells. Figure 9, therefore, quantifies the average phase difference between the CS and SS modulation as a function of stimulus frequency. Note that the average phase lag of the CS modulation with reference to the SS modulation tends to decrease gradually from about −165° at 0.05 Hz to about −155° at 0.8 Hz. In mutant VA-cells, however, the average phase lag of the CS modulation reduced further to about −145° at 0.2 and 0.4 Hz (Student's *t*-test, $P < 0.001$; Wilcoxon rank-sum test, $P < 0.002$). The 95% CI of these differences are listed in the legend. Two-factor ANOVA of these data indicated that there was indeed a significant difference between the two P-cell populations (main effect, $F_{1,175} = 4.43$, $P < 0.002$) and a significant influence of stimulus frequency (main effect, $F_{4,175} = 12.85$, $P < 0.0005$). There were no significant interactions ($F_{4,175} = 1.86$, $P > 0.1$).

As the OKR responses were variable between individual animals (see Fig. 3), the consequent differences in retinal slip across recording sessions might have biased the analysis in Figs 8 and 9. To examine this possibility, we also analysed the phase of the CS modulation with reference to contralaterally directed retinal slip velocity (Fig. 10). It appeared, however, that there were frequency-dependent differences between the two P-cell populations (i.e. significant interactions in two-factor ANOVA; $F_{4,175} = 3.44$, $P = 0.01$). As shown in Fig. 10, the phase of the CS discharge with reference to the retinal slip velocity gradually shifts from an average phase lead of approximately 20° at 0.05 Hz to an average phase lag of about −20° at 0.8 Hz in wild-type P-cells whereas these changes are less steep in mutant P-cells. If the phase curves in Fig. 10 had been identical, it could have been argued that the timing differences observed in Figs 8 and 9 were entirely due to differences in retinal slip rather than differences between the two genotypes. However, the argument cannot be easily reversed. Caution is warranted because nonlinearities in the CS responses, such as complete suppression of

TABLE 3. Regression results of complex spike (CS) modulation

	Stimulus frequency				
	0.05 Hz	0.1 Hz	0.2 Hz	0.4 Hz	0.8 Hz
C57BL/6					
k (spk/s/°)	0.00 ± 0.01	0.05 ± 0.01	0.13 ± 0.02	0.33 ± 0.05	0.67 ± 0.17
r (spk/s per °/s)	−0.66 ± 0.08	−0.55 ± 0.07	−0.71 ± 0.08	−0.78 ± 0.09	−1.01 ± 0.16
n	17	15	28	26	23
L7-PKCI					
k (spk/s/°)	−0.01 ± 0.01	0.06 ± 0.03	0.17 ± 0.02	0.54 ± 0.08	0.84 ± 0.27
r (spk/s per °/s)	−0.71 ± 0.11	−0.46 ± 0.10	−0.47 ± 0.07	−0.84 ± 0.15	−0.92 ± 0.17
n	12	10	23	19	12

Apparent eye position sensitivity (*k*) and apparent eye velocity sensitivity (*r*) for CS responses of floccular Purkinje cells in C57BL/6 wild-type and L7-protein kinase C inhibitor (PKCI) mutant mice. Values of *k* and *r* are expressed as mean ± SEM.

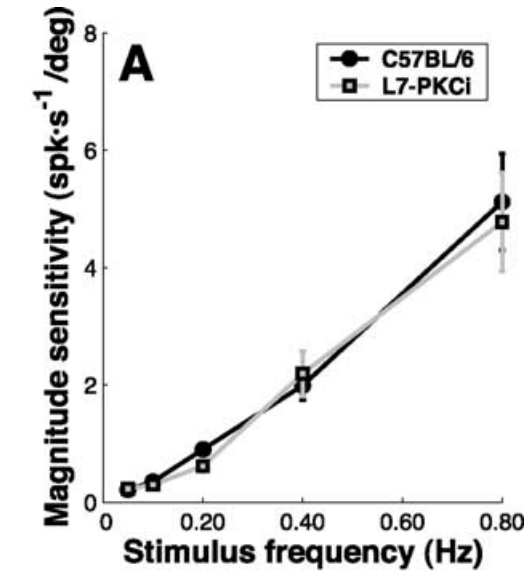

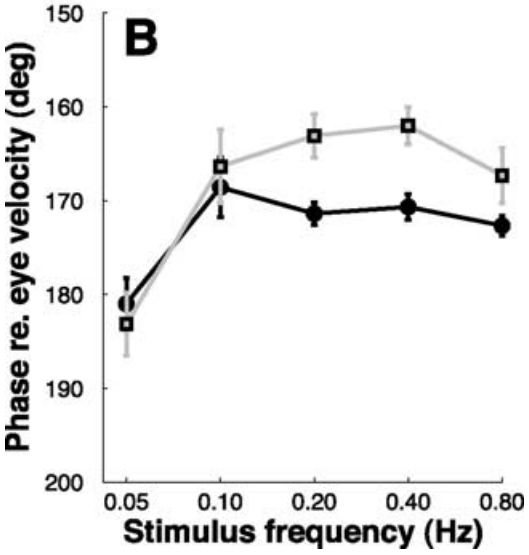

FIG. 8. (A) Magnitude sensitivity and (B) phase of the complex spike discharge of wild-type and mutant Purkinje cells (P-cells) as a function of stimulus frequency. Error bars, ± 1 SEM. Note very similar sensitivity and phase relations for P-cells in C57BL/6 and L7-protein kinase C inhibitor (PKCI) mice. 95% confidence intervals (CI) for the difference between the magnitude sensitivities in the two genotypes are $\Delta M_{0.05} = (-0.06, 0.09)$, $\Delta M_{0.1} = (-0.20, 0.12)$, $\Delta M_{0.2} = (-0.53, 0.03)$, $\Delta M_{0.4} = (-0.63, 1.08)$ and $\Delta M_{0.8} = (-2.5, 1.8)$ spk/s/°. 95% CI for the phase differences between the C57BL/6 and L7-PKCI P-cells are $\Delta\theta_{0.05} = (-10, 6)$, $\Delta\theta_{0.1} = (-8, 11)$, $\Delta\theta_{0.2} = (3, 13)$, $\Delta\theta_{0.4} = (4, 13)$, $\Delta\theta_{0.8} = (-1, 11)°$.

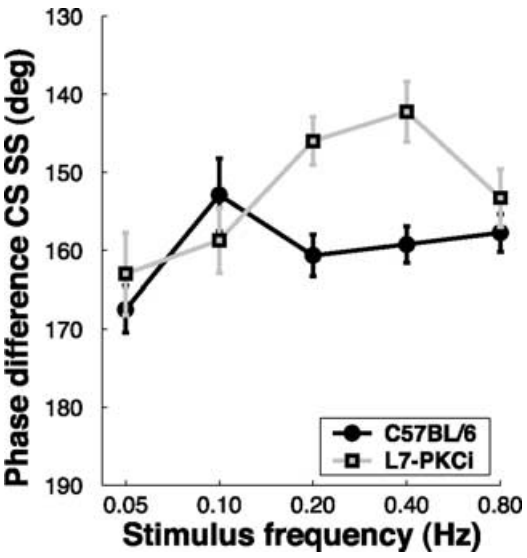

FIG. 9. Average phase of the complex spike (CS) modulation with reference to the simple spike (SS) modulation as a function of stimulus frequency. Error bars, ± 1 SEM. 95% confidence intervals for the phase differences between the two genotypes are $\Delta\theta_{0.05} = (-6, 16)$, $\Delta\theta_{0.1} = (-18, 5)$, $\Delta\theta_{0.2} = (7, 22)$, $\Delta\theta_{0.4} = (8, 25)$, $\Delta\theta_{0.8} = (-3, 13)°$.

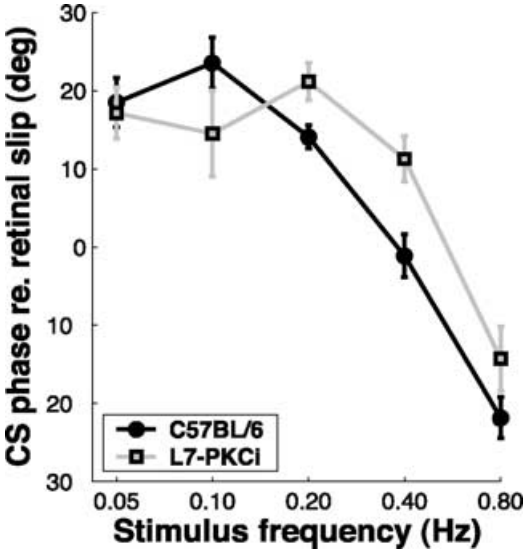

FIG. 10. Average phase of the complex spike (CS) modulation with reference to contralaterally directed retinal slip velocity as a function of stimulus frequency. Error bars, ± 1 SEM. 95% confidence intervals for the phase differences between the two genotypes are $\Delta\theta_{0.05} = (-10, 7)$, $\Delta\theta_{0.1} = (-20, 3)$, $\Delta\theta_{0.2} = (2, 12)$, $\Delta\theta_{0.4} = (5, 20)$, $\Delta\theta_{0.8} = (-2, 16)°$.

the discharge during contralateral stimulus rotation (see Fig. 2 for illustration), suggest that changes in retinal slip could also have a nonlinear effect on the phase of the CS modulation.

Discussion

The main finding of this study is that P-cells in the flocculus of LTD-deficient mice can acquire virtually normal SS and CS discharge dynamics despite the P-cell-specific inhibition of PKC and the consequent blockage of cerebellar LTD from the early stages of development. This result provides a critical extension of our previous work in that it validates the implicit assumption that the normal default oculomotor performance of L7-PKCI mutants is indicative of a proper operation of the cerebellar circuitry (De Zeeuw *et al.*, 1998; Goossens *et al.*, 2001). As discussed below, this extension strongly reinforces the evidence for a causal relation between the lack of LTD induction and the impaired VOR learning in L7-PKCI mutants.

The L7-PKCI transgene is probably activated from the early stages of P-cell differentiation and maturation, resulting in an almost complete suppression of LTD induction throughout pre- and postnatal life

of the animal (De Zeeuw *et al.*, 1998; Goossens *et al.*, 2001). As the development of neural circuits is shaped in part by their activation patterns, these observations raised the interesting question whether P-cells in L7-PKCI mice possess abnormal response properties due to the lack of LTD, which may be one of the mechanisms through which activity-dependent modifications are mediated. Our current results indicate, however, that the SS output of P-cells in LTD-deficient mice is very similar to that in normal ones. First, it appeared that floccular P-cells in L7-PKCI mice exhibit a normal baseline discharge, which agrees well with our recent results obtained from P-cells in the vermis and paramedian lobule (Goossens *et al.*, 2001). Second, we found that the SS discharge dynamics of VA-cells were unaffected. Both the magnitude sensitivity and phase relations were statistically indistinguishable between wild-type and mutant VA-cells. Finally, the CS discharge dynamics were virtually identical between wild-type and transgenic VA-cells, except for a subtle difference in the phase of the CS modulation at some of the applied stimulus frequencies.

Taken together, these findings warrant the conclusion that neither the inhibition of PKC nor the consequent blockage of LTD induction causes fundamental abnormalities in the cerebellar circuitry of L7-PKCI mutant mice. So far, this was merely conjectured on the basis of data showing that L7-PKCI mutants exhibit no deficits in their default oculomotor performance (De Zeeuw *et al.*, 1998; van Alphen & De Zeeuw, 2002) and no general motor coordination deficits (De Zeeuw *et al.*, 1998). The behavioural data alone, however, did not allow for any conclusive inferences regarding the integrity of cerebellar circuitry. In principle, aberrations in the circuit could have been fully masked by compensatory mechanisms in multiple areas of the brain. Clearly, if the discharge dynamics of floccular P-cells had been totally corrupted in the L7-PKCI mutant, there would have been ample reason to argue that the impaired VOR adaptation resulted from fundamental circuit abnormalities rather than from a lack of cerebellar LTD.

Two specific hypotheses have been proposed regarding the neural signals that guide motor learning in the VOR. One suggests that learning in the VOR could be guided by the coincidence of SS firing of P-cells and activity of vestibular inputs to premotor neurons in the vestibular nuclei (Miles & Lisberger, 1981). The other suggests that coincidence of visual climbing fibre and vestibular parallel fibre activity guides learning by inducing LTD of synapses from vestibular parallel fibres to floccular P-cells (Ito, 1982). Although the involved mechanism of synaptic plasticity in the deep cerebellar and vestibular nuclei remains to be uncovered, motor learning in the VOR probably occurs at both sites of plasticity. In view of these hypotheses, it is important to note that the SS signals transmitted to flocculus-receiving neurons in the vestibular nuclei are apparently unaffected in the L7-PKCI mutants as the dynamics of the SS activity of their floccular P-cells appear to be very similar to those in normal animals during the OKR. Of course, we cannot prove that the signals are truly identical; no one can. Nevertheless, it is clear from our present results that the impaired VOR learning in L7-PKCI mutants cannot be explained as a simple side-effect of corrupted SS signals that would functionally disrupt SS-guided motor learning in the brainstem.

Our present results provide no explanation as to why the phase of the CS modulation with reference to the SS modulation is somewhat different between wild-type and L7-PKCI mutant mice at some of the stimulus frequencies. It is known that an olivary subnucleus which provides the climbing fibre inputs to a particular zone of floccular P-cells is, in turn, innervated by the vestibular and/or cerebellar nucleus that is inhibited by that floccular zone (De Zeeuw *et al.*, 1994). Even so, it appears difficult to explain how the activities in such an olivofloccular loop could account for the observed differences in olivary timing and thereby in CS timing, as the SS output of P-cells was unaltered. Perhaps, the small, but significant, difference at 0.2 and 0.4 Hz merely reflects the fact that the CS modulation was nonlinear at these frequencies and that our analysis was, therefore, more susceptible to differences in retinal slip between individual cell recordings. In any case, the observed changes seem to be too subtle ($< 20^{\circ}$) to account for the robust VOR learning deficits found in the L7-PKCI mutant, as they would have a very limited impact on the probability of coincident parallel fibre and climbing fibre inputs.

The fact that the SS output of floccular P-cells is normal in L7-PKCI mutants indirectly supports our tenet that LTD is one of the major mechanisms underlying cerebellar motor learning because it shows that the learning deficits observed in the mutants do not result from abnormal default response patterns. On the other hand, this finding raises the interesting question as to how LTD can have its permanent effect on learning. If LTD modifies the efficacy of the parallel fibre–P-cell synapse to permit learning, it should ultimately influence motor behaviour via a change in SS activities. How can both the SS activities and motor performance be normal in an LTD-deficient mutant? Presumably, SS activation patterns are shaped by a variety of slow- and fast-acting plastic processes that may interact with each other. One can imagine, for example, that parallel fibre LTD is counteracted by postsynaptic long-term potentiation at the same synapse (Lev-Ram *et al.*, 2002) and that these processes collectively determine, via some slower autoregulatory mechanism, the density of α-amino-3-hydroxy-5-methylisoxazole-4-propionate receptors. In this way, the level of LTD induction alone does not determine the absolute efficacy of the synapse in the long run; it would do so only in conjunction with other forms of plasticity. In such a schema, LTD induction could support motor learning both through its immediate (fast-acting) effects on α-amino-3-hydroxy-5-methylisoxazole-4-propionate receptor properties as well as through its (slow-acting) influence on the regulation of α-amino-3-hydroxy-5-methylisoxazole-4-propionate receptor density, but with a different time course. This hypothesis would predict that an impairment of LTD induction affects the speed of learning rather than the ultimate outcome of various training paradigms. This phenomenon was indeed observed when we subjected the L7-PKCI mutants to long periods of VOR adaptation (Van Alphen & De Zeeuw, 2002).

In conclusion, the present findings are the first to show that inhibition of cerebellar LTD induction does not prevent the development of virtually normal P-cell responses during reflex eye movement behaviour in alert L7-PKCI mutants, indicating that their impaired VOR learning cannot be due to fundamental aberrations of the cerebellar circuitry. These results are in line with and re-emphasize our working hypothesis that cerebellar LTD is important for information storage and retrieval in rapid VOR learning (De Zeeuw *et al.*, 1998; Goossens *et al.*, 2001; van Alphen & De Zeeuw, 2002).

Acknowledgements

This research was supported by the Life Sciences Foundation (NWO-ALW/SLW; project no. 805.33.313; A.M.v.A., H.H.L.M.G. and C.I.D.Z.) subsidized by the Netherlands Organization for Scientific Research (NWO), NWO-MW (C.I.D.Z., M.A.F. and J.v.d.S.), Erasmus University Rotterdam (C.I.D.Z., M.A.F. and J.v.d.S.), University of Nijmegen (H.H.L.M.G.), HFSP (C.I.D.Z.) and NIH EY13370 (J.S.S.). We thank B. Weijer and J. v.d. Burg for technical assistance.

Abbreviations

CI, confidence intervals; CS, complex spike; LTD, long-term depression; OKR, optokinetic reflex; P-cell, Purkinje cell; PKC, protein kinase C; PKCI, PKC inhibitor; SS, simple spike; VA-cell, vertical axis P-cell; VOR, vestibulo-ocular reflex.

References

Aiba, A., Kano, M., Chen, C., Stanton, M.E., Fox, G.D., Herrup, K., Zwingman, T.A. & Tonegawa, S. (1994) Deficient cerebellar long-term depression and impaired motor learning in mGluR1 mutant mice. *Cell*, **79**, 377–388.

Conquet, F., Bashir, Z.I., Davies, C.H., Daniel, H., Ferraguti, F., Bordi, F., Franz-Bacon, K., Reggian, A., Matarerse, V., Conde, F. *et al.* (1994) Motor deficit and impairment of synaptic plasticity in mice lacking mGluR1. *Nature*, **372**, 237–242.

De Zeeuw, C.I., Wylie, D.R., DiGiorgi, P.L. & Simpson, J.I. (1994) Projections of individual Purkinje cells of identified zones in the flocculus to the vestibular and cerebellar nuclei in the rabbit. *J. Comp. Neurol.*, **349**, 428–447.

De Zeeuw, C.I., Wylie, D.R., Stahl, J.S. & Simpson, J.I. (1995) Phase relations of Purkinje cells in the rabbit flocculus during compensatory eye movements. *J. Neurophys.*, **75**, 2051–2064.

De Zeeuw, C.I., Hansel, C., Bian, F., Koekkoek, S.K.E., van Alphen, A.M., Linden, D.J. & Oberdick, J. (1998) Expression of a protein kinase C inhibitor in Purkinje cells blocks cerebellar LTD and adaptation of the vestibulo-ocular reflex. *Neuron*, **20**, 495–508.

Eggermont, J.J. (1990) *The Correlative Brain*. Braitenberg, V. (ed.). Springer Verlag, New York.

Frens, M.A., Mathoera, A.L. & van der Steen, J. (2001) Floccular complex spike response to transparent retinal slip. *Neuron*, **30**, 795–801.

Funabiki, K., Mishina, M. & Hirano, T. (1995) Retarded vestibular compensation in mutant mice deficient in δ2 glutamate receptor subunit. *Neuroreport*, **7**, 189–192.

Gao, W., Dunbar, R.L., Chen, G., Reinert, K.C., Oberdick, J. & Ebner, T.J. (2003) Optical imaging of long-term depression in the mouse cerebellar cortex in vivo. *J. Neurosci.*, **23**, 1859–1866.

Goossens, J., Daniel, H., Rancillac, A., van der Steen, J., Oberdick, J., Crépel, F., De Zeeuw, C.I. & Frens, M.A. (2001) Expression of protein kinase C inhibitor blocks cerebellar long-term depression without affection Purkinje cell excitability in alert mice. *J. Neurosci.*, **21**, 5813–5823.

Graf, W., Simpson, J.I. & Leonard, C.S. (1988) Spatial organization of visual messages of the rabbit's cerebellar flocculus. II. Complex and simple spike responses of Purkinje cells. *J. Neurophysiol.*, **60**, 2091–2121.

Ito, M. (1982) Cerebellar control of the vestibulo-ocular reflex. Around the flocculus hypothesis. *Annu. Rev. Neurosci.*, **5**, 275–296.

Ito, M. (1998) Cerebellar learning in the vestibulo-ocular reflex. *TINS*, **2**, 313–321.

Kashiwabuchi, N., Ikeda, K., Araki, K., Hirano, T., Shibuki, K., Tkayama, C., Inoue, Y.L., Kutsuwada, T., Yagi, T. & Kang, Y. (1995) Impairment of motor coordination, Purkinje cells synapse formation, and cerebellar long-term depression in GluRδ2 mutant mice. *Cell*, **81**, 245–252.

Lev-Ram, V., Wong, S.T., Storm, D.R. & Tsien, R.Y. (2002) A new form of cerebellar long-term potentiation is postsynaptic and depends on nitric oxide but not cAMP. *Proc. Natl Acad. Sci. U.S.A.*, **99**, 8389–8393.

Linden, D.J. & Connor, J.A. (1995) Long-term synaptic depression. *Annu. Rev. Neurosci.*, **18**, 319–357.

Lisberger, S.G. (1998) Cerebellar LTD: a molecular mechanism of behavioural learning? *Cell*, **92**, 701–704.

Miles, F.A. & Lisberger, S.G. (1981) Plasticity in the vestibulo-ocular reflex. A new hypothesis. *Annu. Rev. Neurosci.*, **4**, 273–299.

Press, W.H., Flannery, B.P., Teukolsky, S.A. & Vettering, W.T. (1992) *Numerical Recipes in C*, 2nd Edn. Cambridge University Press, Cambridge, MA.

Scheirer, C.J., Ray, W.S. & Hare, N. (1976) The analysis of ranked data derived from completely randomised factorial designs. *Biometrics*, **32**, 429–434.

Shibuki, K., Gomi, H., Chen, L., Bao, S., Kim, J.J., Wakatsuki, H., Fujisaki, T., Fujimoto, K., Katoh, A., Ikeda, T. *et al.* (1996) Deficient cerebellar long-term depression, impaired eyeblink conditioning, and normal motor coordination in GFAP mutant mice. *Neuron*, **16**, 586–599.

Simpson, J.I., Leonard, C.S. & Soodak, R.E. (1988) The accessory optic system of rabbit. II. Spatial organization of direction selectivity. *J. Neurophysiol.*, **60**, 2055–2072.

Simpson, J.I., Wylie, D.R. & De Zeeuw, C.I. (1996) On climbing fiber signals and their consequences. *Beh. Brain Sci.*, **19**, 380–394.

Stahl, J.S. & Simpson, J.I. (1995) Dynamics of abducens nucleus neurons in the awake rabbit. *J. Neurophysiol.*, **73**, 1383–1395.

Van Alphen, A.M., Stahl, J.S. & De Zeeuw, C.I. (2001) The dynamic characteristics of the mouse horizontal vestibulo-ocular and optokinetic response. *Brain Res.*, **890**, 296–305.

Van Alphen, A.M. & De Zeeuw, C.I. (2002) Cerebellar LTD facilitates but is not essential for long-term adaptation of the vestibulo-ocular reflex. *Eur. J. Neurosci.*, **16**, 486–490.